Efficient Plane Detection in Multilevel Surface Maps

V. Prieto-Marañón† J. Cabrera-Gámez†‡ A. C. Domínguez-Brito†‡
vprieto@ono.com jcabrera@dis.ulpgc.es adominguez@iusiani.ulpgc.es
D. Hernández-Sosa†‡ J. Isern-González† E. Fernández-Perdomo†
dhernandez@iusiani.ulpgc.es jisern@iusiani.ulpgc.es enrique.fernandez.perdomo@gmail.com
†Instituto Univ. SIANI. ‡Dpto. de Informática y Sistemas. Univ. de Las Palmas de Gran Canaria

Abstract

An automatic system aimed at producing a compact tridimensional description of indoor environments using a mobile 3D laser scanner is described in this paper. The resulting description is made up of a Multi-Level Surface Map (MLSM) and a series of plane patches extracted from the MLSM. We propose a novel plane detection algorithm, a variant of the efficient RANSAC algorithm, that operates directly over the data structures of a MLSM and does not need to rely on the low level laser data cloud. The mobile 3D scanner is built from a Hokuyo laser range sensor attached to a 2DOF pan-tilt, which is installed on top of a 3DX Pioneer mobile robot. The 3D spatial information acquired by the laser sensor from different poses is used to build a large single map of the environment using the SLAM 6D library. Experimental results demonstrate that the described system is capable of efficiently building compact and accurate 3D representations of complex large indoor environments at multiple semantic levels.

Index Terms-3D Maps, plane detection, multilevel surface maps, laser scanner, SLAM6D

1 Introduction

Efficient use of robots in a tridimensional environment, be it indoor or outdoor, requires identification of structures and objects present in the world. Often these objects and structures can be described in terms of simpler forms or primitives at different semantic levels. Indoors, for example, primitives based on planes can be used to characterize most of the elements conforming the environment. Their descriptions and relative localizations can be used to define the internal representation or map that is to be used by the robots acting in the environment.

Maps are built from information acquired from one or several sensors. There is a big deal of different sensors that can be used to capture information in a 3D scenario like monocular, stereo or time-of-flight cameras, or range sensors, like sonars and lasers. Maps may be topological or metric, but metric maps is the preferred option when geometrical features from the environment, as distances, volumes or surfaces, are needed.

The problem of building maps in large and unknown environments meanwhile the system localizes itself, widely known as the SLAM problem, has been intensively studied by the robotics community during the last ten years [1]. Basically, the problem at hand is to incrementally add new information to a map whilst estimating the relative displacements between observations and recognizing areas that have been already explored and are present in the map. This problem in two dimensions has been largely studied and —in general terms— is nowadays considered solved. The latest achievements in SLAM, together with the availability of faster sensors and processors, have foster the interest for extending the SLAM problem to 3D scenarios with 6DoF observers, a context formerly termed as unfeasible due to its high computational demands.

In the present work, we describe an approach that allows to construct 3D maps for large indoor scenarios using a mobile robotic system equipped with a laser sensor mounted on a pan-tilt unit. The resulting tridimensional representation of the environment comprises two levels of description. At the lowest level, a multilevel map (ML map) [2] is built integrating 3D scans acquired from different poses. To correct from odometry errors, we address the inherent SLAM problem using the SLAM 6D software developed by NÃijchter et al. [3]. From the ML map, the system can detect planes using an algorithm that is an optimized adaptation for plane detection of the efficient RANSAC (eRANSAC) method [4]. These planar patches are used to define a second level of description in the 3D map of the environment from which structures of higher semantic level like walls, doors, tables, etc, could be detected.

This paper is organized as follows: after discussing related works in section 2, the data acquisition system will be described in section 3. The section 4 shows how the ML maps are built. The plane detection algorithm in ML maps will be explained in section 5. Finally, several experimental results and conclusions are discused in sections 6 and 7 respectively.

2 Related work

Different approaches have been developed to allow autonomous mobile robots to build tridimensional maps of the environment. Several methods use a tridimensional grid that splits the space into portions called voxels, whose values reflect the occupancy of the corresponding space volume [5]. Other authors have proposed using elevation maps due to their much lower memory requirements. In elevation maps, the environment is represented by using a two dimensional grid where each cell represents the elevation, i.e. terrain height, at the corresponding point. These maps permit to model large environments as shown in [6]. However, elevation maps are badly suited for modeling scenarios containing structures crossing at different heights over the vertical of a point. Two illustrative examples are a table indoors or a bridge outdoors. In order to avoid this limitation, Triebel et al. [2] propose multilevel surface maps as an extension to elevation maps. These multilevel maps include, at every cell of a bidimensional grid, a list of the traversable surfaces that exist in the corresponding vertical. An improvement of the multilevel surface maps can be found in [7] where they are formally described using a probabilistic approach.

Detecting shapes in tridimensional data sets has been studied from different points of view. Starting from a 3D data point cloud, in [8], a 2 $\frac{1}{2}$ dimensional structure is built based on an incremental triangulation algorithm. Similarly, in [9], the authors develop a plane detection method using a more accurate range noise model for 3D sensors to derive from scratch the expressions for the optimum plane which best fits a point-cloud and for the combined covariance matrix of the planeâĂŹs parameters. The parameters in question are the plane's normal and its distance from the origin. In other works, plane detection is addressed by using the information extracted from imaging sensors. A range imaging sensor is used in [10], with the goal of segmenting images of indoor environments in terms of horizontal and vertical planes by means of the Normalized-Cuts algorithm. An approach by Hähnel, Burgard and Thrun is presented in [11]. This work describes an algorithm for full 3D shape reconstruction of indoor and outdoor environments with mobile robots by approximating environments using flat surfaces. Other authors [12] present a method for obtaining the location, size and shape of main surfaces in an environment from points measured by a laser scanner onboard a mobile robot. The most likely orientation of the surface normal is first calculated at every point, from points in an adaptive-radius neighboring region. In other cases, stereo cameras are used, like in [13], where an architecture for detection and estimation of planar surfaces in the scene from calibrated stereo images is presented.

3 Data acquisition

In this work, the data acquisition system is formed by a laser sensor coupled with a pan-tilt, both installed onboard a mobile robot. The laser sensor is a Hokuyo UTM-30LX with a scan width of 270° and 30m. The pan-tilt unit is a PTU 46-17.5 from Directed Perception. It has two degrees of freedom and it is used for scanning the space in three dimensions. A Pioneer P3-DX has been used as a mobile platform and as the odometry data source.

The data acquisition system works in a move-and-stop way. The robot is moved till a new pose and then a 3D scan is taken. The pan-tilt is oriented with some pan angle α and, then, while the pan-tilt sweeps between the tilt start angle γ_s and the tilt end angle γ_e, the laser sensor takes range measurements from the environment. The laser sensor returns one scan every 25 msecs. The tilt angular speed is adjusted to obtain an angular separation between consecutive scans of ρ degrees at the maximal speed allowed by the hardware.

To integrate new laser measurements into the map we need to know the laser sensor orientation at every moment. A software synchronization mechanism allows to acquire new laser measurements while the pan-tilt is moving between γ_s and γ_e. This synchronization system avoids having to stop the pan-tilt every time the laser begins the acquisition of a new scan. The synchronization algorithm takes into account the pan-tilt's initial position when the laser scan starts and calculates the vertical elevation angle for every measurement returned by the sensor. The scan data timestamp t_s corresponds with the moment at which the laser sensor starts acquiring a new scan. The resolution of the Hokuyo UTM-30LX sensor is 1440 steps per revolution. The timestamp of range measurement m_p corresponding to step p is:

$$t_p = t_s + \frac{p}{1440f} \tag{1}$$

In this equation, f represents the laser beam rotation frequency. Let t_0 be the instant when the pan-tilt began its tilt movement, then, the time difference or delay l_p till the measurement m_p was taken is:

$$l_p = t_p - t_0 \tag{2}$$

The pan-tilt's tilt speed is adjusted so that tilt angle changes in ρ degrees whilst the laser beam completes a revolution. Thus:

$$v = \rho \cdot f \tag{3}$$

Let l_p be known, then, by using a pan-tilt's trapezoidal acceleration scheme, we calculate the tilt angle γ at which each measurement m_p was taken. The pan-tilt uses a trapezoidal acceleration scheme to achieve any velocity that is greater than the so called base speed v_b. It is considered that the pan-tilt unit can accelerate instantaneously from zero to any speed up to v_b. Then γ is calculated by interpolation using this scheme.

The spatial coordinates $c = (c_x, c_y, c_z)$, corresponding to the 3D point where the laser beam impacts, must be calculated for every measurement returned by the laser sensor. Thus, it is necessary to look for a transformation function f such that:

$$c = f(\alpha, \gamma, \lambda, m_p, u) \tag{4}$$

Let λ be the laser motor, i.e. beam, angle and let $u = (u_x, u_y, u_z)$ be the coordinates from the pan-tilt and laser sensor localization. The transformation f can be easily found posing this problem as a direct kinematic problem. From this point of view, our system has three distinct joints. The first and second joints are identified with the pan-tilt's motors. The third joint corresponds to the laser sensor motor, considering the laser beam as another link of the chain (fig. 1). Then, the transformation f can be determined by means of the Denavit-Hartenberg method [14].

3.1 SLAM

As equation 4 clearly shows, it is necessary to know the pan-tilt and laser sensor 3D orientation in order to merge the 3D scans taken from different places in a single map. The localization of each pose is approximated by using

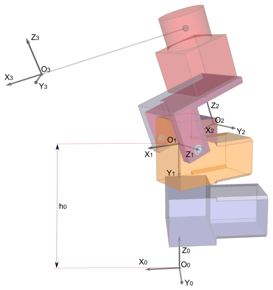

Figure 1: Data acquisition system envisioned as a kinematic chain. The system is made up of a laser sensor (in red color, upper side) coupled over a two degrees of freedom pan-tilt. In the figure, the base reference system is showed.

the robot odometry. However, as it is known, odometry errors might grow without limit due to wheel sleepage or calibration errors. Specifically, one can expect odometry errors to increase rapidly with distance and turns. Hence, it is necessary to correct this error to create a consistent map. For solving this issue, we first collected all 3D scans and then the whole scan set is processed using the SLAM 6D package [3, 15]. The SLAM 6D project includes a software to register 3D point clouds into a common coordinate frame. We use this registration software to correct the localization of the poses. This software matches 3D scans and it considers 6DoF for the robot pose: x, y and z coordinates and the roll, yaw and pitch angles. As a result, corrected poses are returned. We use the corrected poses to solve equation 4.

4 ML map building

The first description level of the environment is based on Multilevel Surface Maps (MLSM) [2] and it is built using the 3D scans processed by the SLAM 6D package.

MLSM consists of a 2D grid where every cell $c_{i,j}$ stores a structure list. Each element of this list is represented as the mean $\mu_{i,j}^k$ and the variance $\sigma_{i,j}^k$ of the measured heights at the position of the cell in the map. The Triebel et al.'s goal in [2] is to obtain an environmental representation that allows robot navigation in tridimensional environments with several traversable surfaces at different overlapped heights. So, in that work, each list element (called surface patches) represents whether the space at the height indicated by the mean $\mu_{i,j}^k$, with an uncertainty equal to the variance $\sigma_{i,j}^k$, is traversable or not. Our objective, however, is to get a map that allows us to model and identify the objects present in the environment. Accordingly, in our map every list element, called block, represents a section of an object surface. This permits to get a map that represents a compact discreatatization of the environment. This new approach introduces some differences during map building.

Within our ML maps, each cell $c_{i,j}$ stores a list of blocks $b_{i,j}^k$. The returned measures $p = (p_x, p_y, p_z)$ are incorporated in a block so $p_x \geq j \cdot \text{cell\_size}$ and $p_x < (j+1) \cdot \text{cell\_size}$ and $p_y \geq i \cdot \text{cell\_size}$ and $p_y < (i+1) \cdot \text{cell\_size}$. The cell_size parameter expresses the map resolution. Every block is represented by a tuple (h, σ, d, π), where h is the height, σ the variance, d the depth and π the plane containing it (this last parameter will be explained in the next section). There are two block types:

1. Horizontal blocks represent a section of the external upper or lower surface in an object, for example: a floor section or a ceil part, a table board, etc. This kind of blocks has a depth equal to zero.

2. Vertical blocks, in turn, represent sections of vertical surfaces of objects like walls or wardrobes.

When new measures are acquired, the height and variance of horizontal blocks will be updated using the Kalman update rule. In vertical blocks, in turn, the height and the variance are the height and variance of the highest measure assigned to the block. The depth of a vertical block is the difference between the upper and lower measures which fit in the block. When new measures are acquired, the map is updated as follows:

- Every time a new measure (p, σ_m), where $p = (p_x, p_y, p_z)$ are the coordinates and

σ_m is the variance corresponding to the measure, the cell $c_{i,j}$ where the measure fits is selected.

- In the block list of the cell $c_{i,j}$ we look for a block (h, σ, d, π) that collects the new measure. A block collects a measure if $|p_z - h| < cell\_size$ and $|(h-d) - p_z| < cell\_size$.
- If there is a block that collects the measure and this block is horizontal and $|p_z - h| < 3 \cdot \sigma$, then the height and variance of the block is updated using the Kalman's update rule. In this case, the block keeps on being horizontal. If, in turn, the block is horizontal but we have that $|p_z - h| \geq 3 \cdot \sigma$, then the block becomes a vertical one with $h = max(p_z, h)$ and $d = |p_z - h|$
- If the block that collects the measure is vertical then we simply update the block height or depth as needed.
- If the new measure is simultaneously collected by two blocks (h_1, σ_1, d_1) and (h_2, σ_2, d_2), then both blocks will be joined in a single vertical block and the old blocks are removed.
- If the measure is not collected by any block, or the block list of the cell is empty, then a new horizontal block will be created with $h = p_z$ and $\sigma = \sigma_m$, and added to the list of cell $c_{i,j}$.

5 Plane detection

We have developed, in this work, an algorithm called efficient Ransac in Multilevel Surface Maps (eRMSM), as a modification of the efficient Ransac (eRansac) algorithm [4]. While eRansac works in point clouds, eRMSM works directly over the block structures of a ML map and it focuses on detecting just planes.

Let M be a ML map that collects a set of blocks $b_{i,j}^k$, so (i, j) is the cell index pair where the block falls in and k is the block index in the cell's list, then the eRMSM algorithm detects and returns a set of planes $\Pi = \{\Pi_1, \cdots, \Pi_n\}$ in the map. Furthermore, each block is labeled with an index i which indicates that the block matches plane Π_i. Matching between a block and a plane implies that the block is close enough to the plane and that the block is part of a block setting with a similar orientation to the plane. When the algorithm stops, each block $b_{i,j}^k$ will be represented as (h, σ, d, π) where π is the index of the matching plane. A block that does not match any plane will have $\pi = 0$.

The algorithm iteratively produces candidate planes (CP) that are hypothesis of real planes. Each CP gets a score, that is defined as a function of the blocks matching the plane. As in eRansa, at the end of each iteration the CP with the highest score is accepted as a valid plane only if the probability of not overlooking a better candidate is high enough. However, in the eRMSM algorithm we have changed the estimation of this probability. In our algorithm, the number of CP needed to accept a plane as valid is strongly reduced as we will demonstrate in the sequel. When a CP Π is accepted as a valid plane, each block that matches the plane is labeled with the index i of the plane. After a CP is accepted, any other CP that matches the accepted plane is removed from the CP list.

Before the algorithm begins, each block $b_{i,j}^k$ receives a direction vector ν. This direction vector will be used so just blocks with a similar direction vector will produce a new CP. This vector is the normal vector to a hypothetic surface formed by the block $b_{i,j}^k$ and all the same kind blocks, vertical or horizontal, in a r radious neighborhood of the block. To speed the process up, in eRMSM we use the Chebyshev distance as the selected distance because it does not change the result. Vector ν is calculated by using the principal component analysis (PCA) [16]. As eRMSM does not work over spatial coordinates, but over map blocks, we must supply, from each block, some coordinates that allow to get a vector $\nu \in \mathbb{R}^3$. Two cases can be differentiated:

- Case 1: the block $b_{i,j}^k$ is horizontal. The horizontal blocks are part of the upper or lower surface from some object like the board in a table, or even the oblique surface from some object like a ramp. So, the direction vector that we are looking for can have any orientation in the space. In this case, from the vertical blocks set $B_V = \{b^{k_1}_{i_1,j_1}, \cdots b^{k_n}_{i_n,j_n}\}$ that exist in a setting with radius r of $b^k_{i,j}$ we can get a point set $P_V = \{p_1, \cdots, p_n\}$ where $p_i \in \mathbb{R}^3$. Let $b^{k_l}_{i_l,j_l} = (h_l, \sigma_l, d_l, \pi_l)$, then the corresponding point p_l is $(i_l \cdot \text{cell\_size}, j_l \cdot \text{cell\_size}, h_l)$. PCA is applied to P_V to compute the normal vector to the surface that has the P_V elements.

- Case 2: the block $b^k_{i,j}$ is vertical. This block must be part of a vertical object: a wall, a chair back, etc. Hence, the direction vector in this block must be a vector parallel to ground then. In this case, from the horizontal blocks set $B_H = \{b^{k_1}_{i_1,j_1}, \cdots b^{k_n}_{i_n,j_n}\}$ that exist in a setting with radius r of $b^k_{i,j}$ we can get a point set $P_H = \{p_1, \cdots, p_n\}$ where $p_i \in \mathbb{R}^2$. Let $b^{k_l}_{i_l,j_l} = (h_l, \sigma_l, d_l, \pi_l)$, then the corresponding point $p_l = (i_l \cdot \text{cell\_size}, j_l \cdot \text{cell\_size})$. PCA is applied to P_H to compute the normal vector (vn_x, vn_y) to the surface that has the P_V elements. Using this two dimensional vector we get the vector $V_N = (vn_x, vn_y, 0)$ which is parallel to ground.

After each block has a direction vector assigned, Algorithm 5 is executed. The candidate planes are generated randomly selecting a block $b^{k_1}_{i_1,j_1}$ and two other blocks $b^{k_2}_{i_2,j_2}$ and $b^{k_3}_{i_3,j_3}$ close to the first that have not been matched to any other accepted plane. The neighborhood radius r is an algorithm's parameter that affects the algorithm's behavior. If r is small, then it is possible that the three blocks are part of the same surface, but the plane's orientation will be affected by measure errors. In other way, if r is big, then the possibility of selecting blocks that do not match the same surface increases, but if the blocks match the same surface, the increased distance will compensate the measurement error. The three selected blocks will generate a CP only if the angles between their direction vectors are lower than a threshold θ.

```
Lp ← ∅ {detected plane list}
Lc ← ∅ {candidate plane list}
FOR i = 0 to Max_cp − 1
    Lc ← Lc ∪ newCandidates(r, θ)
    b ← bestCandidate(Lc)
    sc ← SimilarOrientationSurface(b)
    IF P(surface(b), sc) > pt
    %matching blocks are removed:
        M ← M − Mb
        Lp ← Lp ∪ b
    %CP that matches b are removed:
        Lc ← Lc − Cm
    END IF
END FOR
```

Algoritmo 1: Plane detection in a ML map M.

In the eRANSAC algorithm, the CP is determined as the plane that includes the three selected points (see fig. 2 (a) and (b)). Contrary, to filter the surface localization error due to measurement errors, our method determines the CP in other way. The plane that is generated from the three blocks CP cp_i is determined as a point o and a normal vector to plane V_N. The point o is selected as the barycenter of the polygon with the three blocks as vertex and the normal vector V_N as the mean between the corresponding direction vectors. Such a CP represents a better hypothesis of a real plane (fig. 2 c).

The way a score is assigned to each CP in eRMSM algorithm also varies in relation to previous works. Since our algorithm works with blocks, instead of point clouds, it is not possible to assign the number of matching points to CP as score, so we propose a new score function. Now, we are going to give a definition of matching between a block and a plane. It is said that a block $b^k_{i,j}$ with a direction vector V_D matches a plane $\Pi = (o, V_N)$ if:

- The distance from the block to the plane is $d = dist(b^k_{i,j}, \Pi) < \varepsilon$.
- The angle between the block's direction vector and the normal vector to the plane

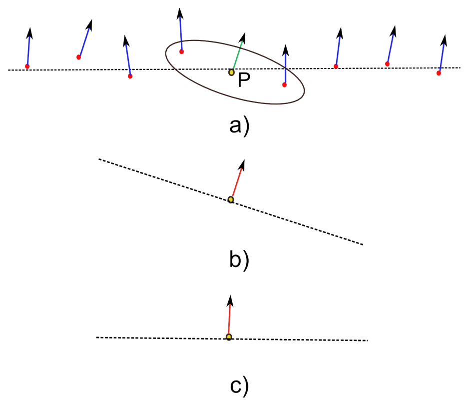

Figure 2: Different ways to determine a candidate plane. At the figure, by simplicity, we can see the problem in two dimensions form. a) Measures set of a straight line. b) Determining a candidate line as the line with minimal distance to three neighbor points. c) Determining a candidate line as the line with a normal vector that is the mean of the direction vectors of the three points.

is $\beta = \arg(V_D, V_N) < \kappa$.

The thresholds ε and κ are system parameters that adjust the goodness of the accepted CP as valid planes.

Each CP receives a score in function of the area of the surface that is represented by the blocks that match that plane. To normalize the probabilistic computations, the area is measured in “surface units" s_u, where $s_u = \text{cell\_size} \times \text{cell\_size}\ \text{mm}^2$. Then the CP score is $S = \sum s_{b_i}$, where s_{b_i} is the area of the surface represented by the blocks matching the plane. The block surface depends on the kind of block: vertical or horizontal. In a vertical block b_v the corresponding surface is $s_v = \frac{d}{\text{cell\_size}}$. When the block is horizontal it has a surface $s_h = 1$. This score method, instead of counting the number of matching blocks, as in the original method, has the advantage of being based on a real indicator of the importance of the plane in the real world. Hence, a CP that corresponds to a large surface has more possibilities of being found early.

A CP is accepted as valid only if the probability of not overlooking a better candidate is high enough. As we can see in [4], let $\wp$ be a cloud of N data points and let Ψ be a shape comprising n points, then the probability of detecting Ψ in a single iteration is

$$P(n) = \binom{n}{k} / \binom{N}{k} \approx \left(\frac{n}{N}\right)^k \qquad (5)$$

Let k be the minimal number of elements needed to define a shape —$k = 3$ for planes— thus, the probability $P(n, s)$ of successfully detecting a shape after s new candidates have been generated is

$$P(n, s) = 1 - (1 - P(n))^s \qquad (6)$$

At last, the number T of needed candidates to detect a shape of a size n with a probability $P(n, T) \geq p_t$, where p_t is the minimal desired probability, is

$$T \geq \frac{\ln(1 - p_t)}{\ln(1 - P(n))} \qquad (7)$$

Let equations 5, 6 and 7, and suppose that we have as environment a corner formed by a ground section and two walls. Let the number of points in the cloud be equally spread over the three planes. Hence, each plane has a third part of the total points. Then, as 5 shows, the probability to detect the ground in a single pass is:

$$P(n) \approx \left(\frac{1}{3}\right)^3 \approx 0.037 \qquad (8)$$

Hence, according to equation 7, the number of CP that we need to detect the ground with a probability greater or equal to 0.99 is:

$$T \geq \frac{\ln(1 - 0.99)}{\ln(1 - 0.037)} > 122 \qquad (9)$$

Clearly, with other shapes that represent less than a third part of the total information, the number of candidates are highly increased as usually happens in realistic environments, where most surface planes represent little portion of the total map. In the eRMSM algorithm, we have introduced changes to estimate the probability of not overlooking a better candidate. These changes highly reduce the number of CP that is necessary to generate before a plane is accepted as valid.

In our approach, CP are not generated from any three blocks of the map. On the contrary, each CP is exclusively generated from three neighbor blocks with a similar orientation and therefore similar to the orientation that the plane itself will have. Exploiting that fact, in eRMSM algorithm, let Π be a CP where s_c is the surface of the matching blocks to the plane and let s_o be the total surface of all blocks with a similar orientation to Π, we calculate the probability to find the plane in a single pass as

$$P(s_c) = \binom{s_c}{3} / \binom{s_o}{3} \approx \left(\frac{s_c}{s_o}\right)^3 \qquad (10)$$

In the example of three planes forming a corner, the probability of finding the plane corresponding to the ground in a single pass is 1, since $s_c = s_o$ and then

$$P(s_c) \approx \left(\frac{s_c}{s_o}\right)^3 = (1)^3 = 1 \qquad (11)$$

In this case, we have enough with only a single generated CP against the 123 needed candidates using the previous approach. This method can validate CP spurious planes or planes with little significance, i. e. with a small total surface if the matching blocks to the plane represent a high percentage of all blocks with an orientation equal or similar to the generated CP. To avoid this, it suffices with a threshold accepting candidate planes only with a score greater than a value s_m and thence with a minimal surface.

The algorithm exit condition is reached when a given number of candidates is generated.

6 Results

The system presented in this paper has been tested in several localizations of the main building of the Universidad de Las Palmas de Gran Canaria's Technological Park. In the first test, we steered the robot over the basement and took 24 3D scans of the corridor (see fig. 3(a)). The corridor's estimated dimensions are 40.5m length and 4.75m wide.

(a)

(b)

Figure 3: (a) Test scenario 1: Corridor of the Technological Park. ULPGC. (b) Test scenario 2: Robotic laboratory at the Technological Park. ULPGC.

The corridor has perpendicular subcorridors of 11m length.

We used the NÃijchter et al. SLAM 6D library [3] to correct the odometer localization information returned by the robot regarding the robot's pose where the 24 3D scans where taken. Once the poses are corrected, we build a map from the set of measures taken in the 3D scans. A 3D visualization software was developed to make spatial zooms and rotations of the map. In fig. 4 we can see an upper oblique view from a map of the corridor generated using a 100mm cell size. For better visualization we have removed the floor and the ceiling from the map. In addition, we can see the poses where the 3D scans were taken from. This map allocates 44732 blocks.

Once the map is generated, the eRMSM algorithm is executed. With an implementation of the algorithm optimized for a 2.4GHz quad-core processor, it is possible to identify 12 planes in 7.8 seconds. In figure 5 we can see the corridor map where the blocks that match any detected plane are depicted using different

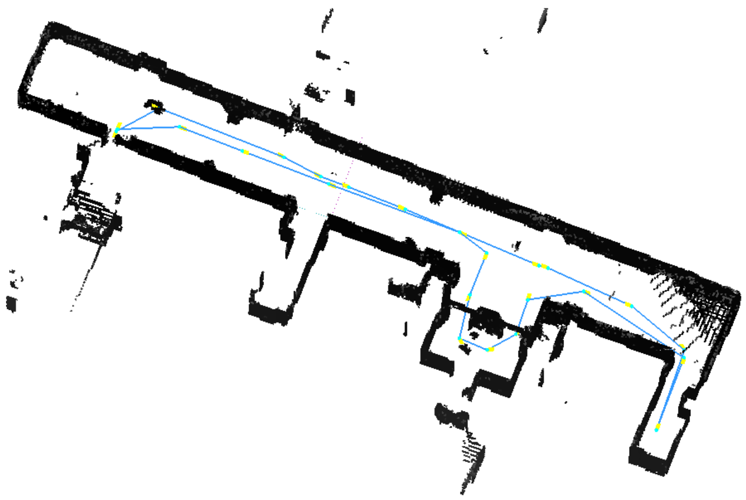

Figure 4: Upper oblique view of multilevel surface maps generated from 24 poses at the corridor. The line in the map is the robot trajectory and the points over the line are the poses at which the scans were taken.

colors. The largest planes in this map match about 1650 blocks. Using the eRansac test it would be needed to generate 1132 CP (see equation 7) to accept the first plane with a probability greater than 0.9. Using our probability estimation, the first plane hypothesis is confirmed after generating 50 CP in 600ms.

Figure 3(b) shows a new test scene. In this case, the stage is a robotic laboratory 8.3m wide and 11.4m length. Figure 6(a) shows a map generated using a 20mm cell size. This map collects 196385 blocks. As in the previous test, different colors in figure 6(b) correspond with blocks that match different detected planes.

ML maps, in the way we have generated them, easily allow the joining or fusion of different partial maps of adjacent spaces. The laboratory showed in figure 3(b) and the corridor of figure 3(a) are contiguous rooms in the same building. Both spaces were independently mapped using our approach (shown in figure 6(a) and 4. We have been able to generate a single map from both data sets after the poses were corrected using the SLAM 6D software. We can see the resulting map in figure 7.

7 Conclusions

This paper has described an approach for building compact 3D maps of indoor environments based on multilevel surface maps. This kind of space representation allows to describe the scene with detail andÂăbalances spatial resolution and memory cost adequately. These multilevel maps are easily scalable and versatile enough to provide sophisticated spatial information without having to rely on low level data, i.e. clouds of laser data points.

In addition, an efficient algorithm for detecting planes using the multilevel surface maps (eRSMS algorithm) has been proposed. A key feature of the eRSMS algorithm, that distinguishes it from the original eRANSAC algorithm, is that it does not need to generate a high number of hypothesis in order to identify candidate planes with high probability. Moreover, eRSMS is easily parallelizable, an attractive feature that may be exploited on multicore processors.

While the system described in this paper has proved reliable, there is a large margin for improvement. Future work will be directed towards alleviating the off-line 6D SLAM preprocessing and the associated computational

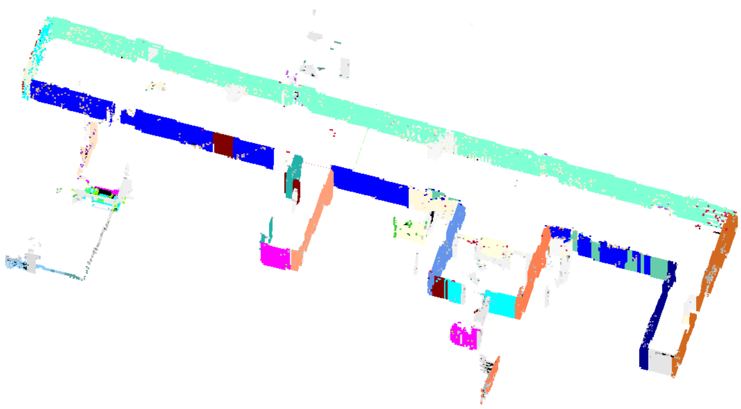

Figure 5: Detected planes in the corridor map. Grey zones represent blocks that do not match any plane. Each color represents different detected planes.

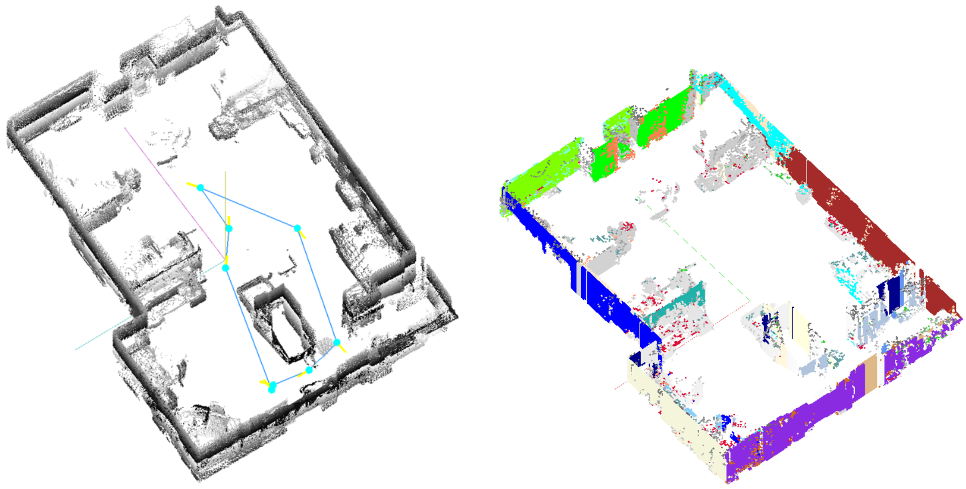

(a) (b)

Figure 6: (a) Upper oblique view of multilevel surface maps generated from 8 poses at the Robotic's laboratory. The line in the map is the robot trajectory and the points over the line are the poses at which the scans were taken. (b) Detected planes in the laboratory map. Grey zones represent blocks that do not match any plane. Each color represents different detected planes.

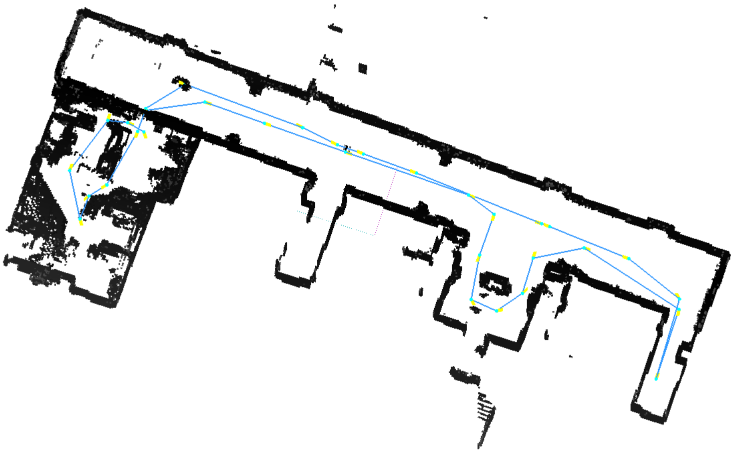

Figure 7: This single map of the corridor and the Robotic's laboratory all together was generated from the independent scans of both stages.

cost by using geometrical features instead of the scan data points. Also the multilevel maps offer interesting possibilities for attempting a semantic labelling of an indoor space.

8 Acknowledgements

This work has been partially supported by the Research Project *TIN2008-06068* funded by the Ministerio de Ciencia e Innovación, Gobierno de España, Spain.

References

[1] Josep Aulinas, Yvan Petillot, Joaquim Salvi, and Xavier Lladó. The SLAM problem: a survey. In *Proceeding of the 2008 conference on Artificial Intelligence Research and Development*, pages 363–371, Amsterdam, The Netherlands, The Netherlands, 2008. IOS Press.

[2] Rudolph Triebel, Patrick Pfaff, and Wolfram Burgard. Multi-level surface maps for outdoor terrain mapping and loop closing. In *In Proc. of the IEEE/RSJ Int. Conf. on Intelligent Robots and Systems (IROS)*, 2006.

[3] Andreas Nüchter, Kai Lingemann, and Joachim Hertzberg. 6D SLAM with cached K-D tree search. In *RA '07: Proceedings of the 13th IASTED International Conference on Robotics and Applications*, pages 101–106, Anaheim, CA, USA, 2007. ACTA Press.

[4] Ruwen Schnabel, Roland Wahl, and Reinhard Klein. Efficient RANSAC for Point-Cloud Shape Detection. *Computer Graphics Forum*, 26(2):214–226, June 2007.

[5] Julian Ryde and Michael Brünig. Non-cubic occupied voxel lists for robot maps. In *IROS'09: Proceedings of the 2009 IEEE/RSJ international conference on Intelligent robots and systems*, pages 4771–4776, Piscataway, NJ, USA, 2009. IEEE Press.

[6] Shrihari Vasudevan, Fabio Ramos, Eric Nettleton, and Hugh Durrant-Whyte. Gaussian process modeling of large-scale terrain. *J. Field Robot.*, 26(10):812–840, 2009.

[7] Cesar Rivadeneyra, Isaac Miller, Jonathan R. Schoenberg, and Mark Campbell. Probabilistic estimation

of multi-level terrain maps", booktitle = "ICRA'09: Proceedings of the 2009 IEEE international conference on Robotics and Automation. pages 3709–3714, Piscataway, NJ, USA, 2009. IEEE Press.

[8] Zoltan Csaba Marton, Radu Bogdan Rusu, and Michael Beetz. On fast surface reconstruction methods for large and noisy point clouds. In *ICRA'09: Proceedings of the 2009 IEEE international conference on Robotics and Automation*, pages 2829–2834, Piscataway, NJ, USA, 2009. IEEE Press.

[9] Kaustubh Pathak, Narunas Vaskevicius, and Andreas Birk. Revisiting uncertainty analysis for optimum planes extracted from 3D range sensor point-clouds. In *ICRA'09: Proceedings of the 2009 IEEE international conference on Robotics and Automation*, pages 2035–2040, Piscataway, NJ, USA, 2009. IEEE Press.

[10] GuruPrasad M. Hegde and Cang Ye. Extraction of planar features from swissranger sr-3000 range images by a clustering method using normalized cuts. In *IROS'09: Proceedings of the 2009 IEEE/RSJ international conference on Intelligent robots and systems*, pages 4034–4039, Piscataway, NJ, USA, 2009. IEEE Press.

[11] D. Hähnel, W. Burgard, and S. Thrun. Learning compact 3d models of indoor and outdoor environments with a mobile robot. *Robotics and Autonomous Systems*, 44(1):15–27, 2003.

[12] Mariano Martin Nevado, Jaime Gomez Garcia-Bermejo, and Eduardo Zalama Casanova. Obtaining 3d models of indoor environments with a mobile robot by estimating local surface directions. In *Robotics and Autonomous Systems, 48:131 âĂŞ 143*, pages 131–143, 2004.

[13] Martin Heracles, Bram Bolder, and Christian Goerick. Fast detection of arbitrary planar surfaces from unreliable 3D data. In *IROS'09: Proceedings of the 2009 IEEE/RSJ international conference on Intelligent robots and systems*, pages 5717–5724, Piscataway, NJ, USA, 2009. IEEE Press.

[14] J. Denavit and R. S. Hartenberg. A kinematic notation for lower-pair mechanisms based on matrices. *Trans ASME J. Appl. Mech*, 23:215–221, 1955.

[15] Andreas Nüchter and K. Lingemann. 6D Simultaneous Localization and Mapping, 2010. http://slam6d.sourceforge.net/.

[16] I.T. Jolliffe. *Principal Component Analysis*. Springer, New York, NY, 1986.